Nested Silicon Microring Resonator with Multiple Coupling Regimes

Jiayang Wu, Zhiming Zhuang, Mu Xu, Pan Cao, Xinhong Jiang, Linjie Zhou, and Yikai Su
State Key Laboratory of Advanced Optical Communication Systems and Networks, Department of Electronic Engineering, Shanghai Jiao Tong University, Shanghai 200240, China, E-mail: yikaisu@sjtu.edu.cn

Abstract — **We propose and demonstrate a nested silicon microring resonator that realizes multiple coupling regimes at different resonance wavelengths in one passive device. Resonance notches with diverse depths and bandwidths in the transmission intensity spectrum can be experimentally achieved, which demonstrates the intensity responses of multiple coupling regimes. Moreover, the phase responses of multiple coupling regimes is also verified by observing fast or slow lights at different resonance wavelengths.**

Keywords- microring resonator, multiple coupling regimes

I. INTRODUCTION

Silicon microring resonators (MRRs) are promising building blocks for future photonic integrated circuits. For a typical single MRR consisting of a microring side coupled to a straight waveguide, there could be three coupling regimes depending on the balance between the waveguide coupling and the intrinsic cavity loss, namely over coupling, critical coupling and under coupling regimes. Each regime has its own distinct intensity and phase response [1]. With these three coupling regimes, various applications of optical signal processing such as fast/slow light [2], [3], intensity/phase modulation [4] have been proposed.

However, it is difficult to realize all these three coupling regimes in a single MRR since both the waveguide coupling and the intrinsic cavity loss are almost fixed once a passive device has been fabricated. Moreover, it is also difficult to control the fabrication to achieve a specific coupling regime, especially the quasi-critical coupling. To solve this problem, some schemes based on active modulation have been proposed [5], [6]. Although they achieve multiple coupling regimes, the stringent requirements to design and fabricate electrical modulation modules may bring additional complexity. In this paper, we propose a nested silicon MRR that realizes multiple coupling regimes in one passive device. For different resonance notches of the transmission intensity spectrum, diverse notch depths and bandwidths owing to multiple coupling regimes can be theoretically designed and practically achieved. The phase response is also investigated, with experimental observation of fast/slow lights at different resonance wavelengths further proving the realization of multiple coupling regimes.

II. DEVICE STRUCTURE AND OPERATION PRINCIPLE

Fig. 1(a) illustrates the schematic of the configuration that we propose: a microring is nested inside a U-bend waveguide to form a larger resonant loop, and another bus waveguide side coupled to the bottom of the U-bend waveguide acts as system input /output. From the transfer function of the drop port of the add-drop MRR, we obtain the relation between E_3 and E_4 (depicted in Fig.1) as follows:

$$\frac{E_3}{E_4}=\frac{-\kappa_2^2 a_1^2 a_2 e^{i(2\varphi_1+\varphi_2)}}{1-r_2^2 a_2^2 e^{i(2\varphi_2)}}=|A|e^{i\Phi}, \tag{1}$$

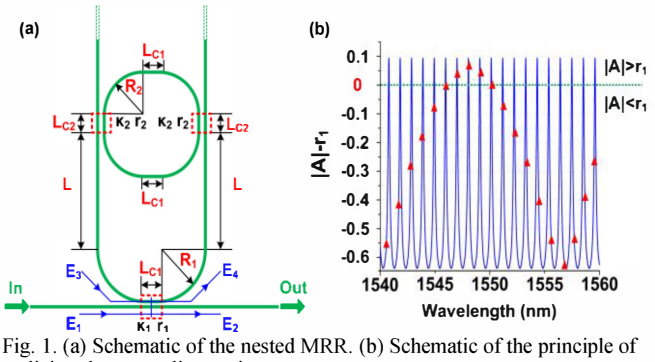

Fig. 1. (a) Schematic of the nested MRR. (b) Schematic of the principle of realizing three coupling regimes.

where $|A|$ and Φ are the amplitude and phase of the complex ratio, respectively. Then the transfer function of the proposed configuration can be written as:

$$\frac{E_2}{E_1}=\frac{r_1-|A|e^{i\Phi}}{1-r_1|A|e^{i\Phi}}=\frac{r_1-r_1r_2^2a_2^2e^{i(2\varphi_2)}+\kappa_2^2a_1^2a_2e^{i(2\varphi_1+\varphi_2)}}{1-r_2^2a_2^2e^{i(2\varphi_2)}+r_1\kappa_2^2a_1^2a_2e^{i(2\varphi_1+\varphi_2)}}, \tag{2}$$

in both (1) and (2), r_i and κ_i (i=1,2) are the transmission and cross-coupling coefficients of the two kinds of couplers, respectively; $\varphi_{1,2}=kL_{1,2}$, with k denoting the propagation constant, are the phase changes associated with the waveguides with lengths of $L_1=(\pi R_1+L_{c1}+L_{c2})/2+L$ (half length of the U-bend waveguide) and $L_2=\pi R_2+L_{c1}+L_{c2}$ (half circumference of the nested microring); and $a_{1,2}=\exp(-\alpha L_{1,2}/2)$, with α denoting the loss factor, are the transmission factors associated with the waveguides with lengths of $L_{1,2}$.

For low loss and strong coupling condition, we assume $r_1=r_2=0.825$, α=80/m, and n_g=4.335 as the group index. Then we choose the structural parameters that meet this condition as follows: $L_{c1}=L_{c2}$=7 μm, R_2=80 μm, R_1=80.63 μm with added waveguide width of 0.45 μm and added slot width of 0.18 μm, and L=248 μm. With these parameters, we plot $|A|$-r_1 that is obtained from (1) in the wavelength range of 1540 nm~1560 nm in Fig. 1(b). The resonance wavelengths that satisfy $\Phi=2m\pi$ (m is an integer) are also shown by the red triangles on the curve. If we regard the proposed nested configuration as an equivalent single MRR, r_1, $|A|$ and Φ are the equivalent transmission coefficient, round-trip transmission factor, and round-trip phase, respectively. In different cases of $|A|>r_1$, $|A|=r_1$ and $|A|<r_1$, multiple coupling regimes of over coupling, critical coupling and under coupling can be achieved correspondingly. From Fig. 1(b) one can see that some triangles lie in the region of $|A|>r_1$; while some others are in the region of $|A|<r_1$; particularly, several triangles almost lie on the dividing line, meaning that the corresponding multiple coupling regimes can be achieved at different resonance wavelengths.

III. DEVICE FABRICATION AND MEASURED SPECTRUM

Based on the above principle, the designed device is fabricated on an 8-inch SOI wafer. A micrograph of the

fabricated device is shown in Fig. 2(a). 248-nm deep ultraviolet photolithography is used to define the pattern and inductively coupled plasma etching process is used to etch the top silicon layer. The structural parameters are in accordance with previous discussion. Grating couplers are employed at each end to couple light into/out of chip with single-mode fibers.

The spectral response of normalized transmission intensity measured with the fabricated device is shown in Fig. 2(b) by the blue solid curve. TABLE I presents the measured depths and bandwidths of different resonance notches. The measured curve is then fitted by the red dashed curve obtained from (2) with fitting parameters of r_1=r_2≈0.8232, α≈72/m, n_g≈4.17395, which are close to the parameters we used for the design. From Fig. 2(b) one can see that the measured curve fits well with the one obtained from (2), except for slight decay on the left edge, which could be attributed to the limited transmission bandwidth of the grating couplers.

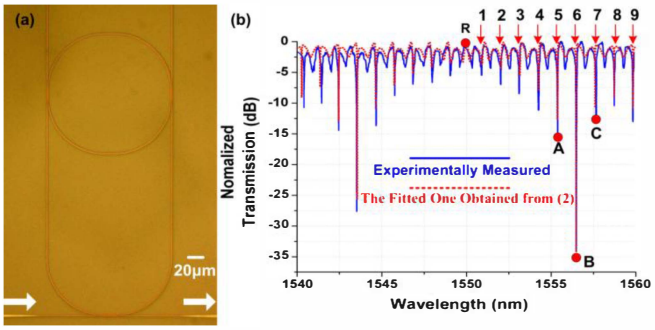

Fig. 2. (a) Micrograph of the fabricated device. (b) Experimentally measured transmission intensity spectrum (blue solid curve) and the fitted one obtained from (2) (red dashed curve).

TABLE I. Depth, Bandwidth for the Notches in Fig. 2(b)

Notch number	1	2	3	4	5	6	7	8	9
Notch depth (dB)	5.8	7.1	8.5	11.5	15	35.2	12.7	10.5	12.8
Notch 3-dB bandwidth (nm)	0.093	0.090	0.085	0.076	0.068	0.048	0.043	0.037	0.041

IV. Fast/Slow Lights Experiment

In the case of the over coupling regime, the dispersion-induced group delay (GD) is positive to produce slow light. On the other hand, GD is negative in the under coupling regime to produce fast light. We perform a fast/slow lights experiment using the fabricated device to demonstrate the phase responses of multiple coupling regimes. The experimental setup is shown in Fig. 3. A 5-Gb/s RZ pulse train with a duty cycle of 50% is generated by two cascaded MZMs. We tune the wavelength of the CW light to measure

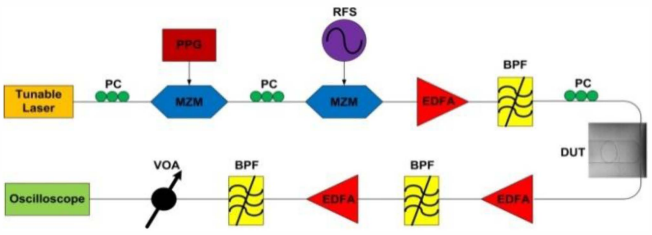

Fig. 3. Experimental setup for the observation of fast/slow lights. MZM: Mach-Zehnder Modulators, PC: Polarization Controller, PPG: Pulse Pattern Generator, RFS: Radio Frequency Source, BPF: Band Pass Filter, DUT: Device Under Test, VOA: Variable Optical Attenuator.

the pulse advancement or delay. As shown in Fig. 2(b), points A, B and C correspond to three different wavelengths at different resonance notches; point R corresponds to the reference wavelength out of the notches. Firstly, we set the signal wavelength off-resonance at point R and take the corresponding pulse waveform as the reference, shown in Fig. 4 by curve R. Then the wavelength is tuned to the resonance notch at point A, we observe that the pulse is advanced by ~32 ps, as shown in Fig. 4 by curve A. When the wavelength is tuned to another resonance notch at point C, a pulse delay of ~84 ps can be observed, as shown in Fig. 4 by curve C. Particularly, when the wavelength is tuned to the deepest notch at point B, a waveform similar to that in [7] with pulse-splitting can be observed, as shown in Fig. 4 by curve B, which indicates the approaching of the critical coupling condition.

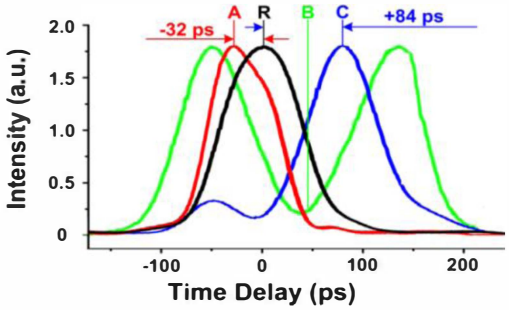

Fig. 4. Experimentally measured temporal waveform of 5 Gb/s RZ pulse at different resonance wavelengths in Fig. 2(b).

V. Conclusion

In conclusion, we propose a nested silicon MRR with three coupling regimes of over coupling, under coupling and quasi-critical coupling in one passive device. In the transmission intensity spectrum, resonance notches with diverse depths and bandwidths are theoretically designed and experimentally achieved. The phase responses of multiple coupling regimes are also verified by the observing fast/slow lights and pulse-splitting at different resonance wavelengths.

VI. Acknowledgement

This work was supported in part by NSFC (61077052/61125504/61235007), MoE (20110073110012), and Science and Technology Commission of Shanghai Municipality (11530700400).

References

[1] S. Feng, T. Lei, H. Chen, H. Cai, X. Luo, and A. W. Poon, "Silicon photonics: from a microresonator perspective, "*Laser Photonic Rev.*, vol. 6, no. 2, pp. 145-177, 2012.

[2] Q. Li, Z. Zhang, J. Wang, M. Qiu, and Y. Su, "Fast light in silicon ring resonator with resonance-splitting," *Opt. Exp.*, vol. 17, no. 2, pp. 933-940, 2009.

[3] F. Liu, Q. Li, Z. Zhang, M. Qiu and Y. Su, "Optically tunable delay line in silicon microring resonator based on thermal nonlinear effect," *IEEE J. Sel. Top. Quantum. Electron.*, vol. 14, no.3, pp. 706-712, 2008

[4] T. Ye, Y. Zhou, C. Yan, Y. Li and Y. Su, "Chirp-free optical modulation using a silicon push–pull coupling microring," *Opt. Lett.*, vol. 34, no. 6, pp.785-787, 2009.

[5] W. Sacher, W. Green, S. Assefa, T. Barwicz, H. Pan, S. Shank, Y. Vlasov, and J. Poon, "28 Gb/s silicon microring modulation beyond the linewidth limit by coupling modulation," OFC/NFOEC, OM3J.2, 2012.

[6] M. Chang, M. Lee and M. C. Wu, "Tunable coupling regimes of silicon microdisk resonators using MEMS actuators," *Opt. Exp.*, vol. 14, no. 11, pp. 4703-4712, 2006.

[7] F. Liu, T. Wang, Q. Li, T. Ye, Z. Zhang, M. Qiu, and Y. Su, "Compact optical temporal differentiator based on silicon microring resonator", *Opt. Exp.*, vol. 16, No. 20, pp. 15880-15886, 2008.